Antarctic Ice Sheet elevation impacts on water isotope records during the Last Interglacial

Sentia Goursaud[1], Max Daniel Holloway[2], Louise C Sime[2], Eric W. Wolff[1], Paul Valdes[3], Eric J. Steig[4], and Andrew George Pauling[4]

[1]University of Cambridge
[2]British Antarctic Survey
[3]University of Bristol
[4]University of Washington

November 23, 2022

Abstract

Knowledge of how the Antarctic Ice Sheet (AIS) has varied in response to past climates can inform the prediction of future AIS behaviour. Water stable isotope records from Antarctic ice cores traditionally provide information on past temperature changes. However, these reconstructions neglect changes in atmospheric circulation, which can be induced by elevation changes. Here, we simulate an ensemble of idealised AIS elevation change scenarios using the isotope-enabled HadCM3 climate model during the Last Interglacial period (LIG). Our ensemble is used to investigate the isotope-elevation relationship. Changing AIS elevations linearly modify the response in surface air temperature, as precipitation and δ^{18}O. Especially, we observe δ^{18}O decrease with the AIS elevation, with higher slopes on the coast compared to the plateau, reflecting different processes. We note that the effect of sea-ice induced by AIS changes is small. These results help to isolate the effect of AIS changes on the LIG δ^{18}O signals.

Antarctic Ice Sheet elevation impacts on water isotope records during the Last Interglacial

Sentia Goursaud[1], Max Holloway[2], Louise Sime[3], Eric Wolff[1], Paul Valdes[4], Eric Steig[5], Andrew Pauling[5]

[1]Department of Earth Sciences, University of Cambridge, UK
[2]Scottish Association for Marine Science, Oban, UK
[3]Ice Dynamics and Paleoclimate, British Antarctic Survey, Cambridge, UK
[4]School of Geographical Science, University of Bristol, Bristol, UK
[5]Department of Atmospheric Sciences, University of Washington, Seattle, US

Key Points:

- Lowering the Antarctic Ice Sheet during the Last Interglacial increases the water stable isotopes in the precipitations.
- An isotopic linear response to Antarctic Ice Sheet elevation changes during the Last Interglacial can be extracted.
- The effect of the elevation-induced sea-ice on water stable isotopes are small so the effect of the elevation can be isolated.

Corresponding author: Sentia Goursaud, `sg952@cam.ac.uk`

Abstract

Knowledge of how the Antarctic Ice Sheet (AIS) has varied in response to past climates can inform the prediction of future AIS behaviour. Water stable isotope records from Antarctic ice cores traditionally provide information on past temperature changes. However, these reconstructions neglect changes in atmospheric circulation, which can be induced by elevation changes. Here, we simulate an ensemble of idealised AIS elevation change scenarios using the isotope-enabled HadCM3 climate model during the Last Interglacial period (LIG). Our ensemble is used to investigate the isotope-elevation relationship. Changing AIS elevations linearly modify the response in surface air temperature, as precipitation and δ^{18}O. Especially, we observe δ^{18}O decrease with the AIS elevation, with higher slopes on the coast compared to the plateau, reflecting different processes. We note that the effect of sea-ice induced by AIS changes is small. These results help to isolate the effect of AIS changes on the LIG δ^{18}O signals.

Plain Language Summary

The Last Interglacial period (LIG, 128 kyears BP) was at least 2 °C warmer than today. It is a prime example for studying the consequences of future global temperature rise, especially of sea level rise through polar ice cap melting. Through the scope of analyses, records of water stable isotopes from Antarctic ice cores are classically used to reconstruct past surface temperatures. However a couple of underlying hypotheses are made, including no changes in the elevation and sea-ice extent. Thus in this manuscript, we studyed the effect of the Antarctic Ice Sheet (AIS) elevation on water stable isotopes in precipitations, using an ensemble of climate simulations where we varied the AIS elevation. We observed that (i) water stable isotopes lowers with the AIS elevation following linear relationships, (ii) the effect of sea-ice induced by AIS elevation is small so the effect of AIS elevation can be isolated. Finally, this study brings an extended knowledge of the different effects on water stable isotopes recorded in Antarctic ice core covering the LIG period, which are to be taken into account to extract a realistic climatic information.

1 Introduction

Geological data indicate that the West Antarctic Ice Sheet (WAIS) expanded beyond its present-day configuration during the Last Glacial Maximum (LGM; approximately 21 kyears BP (ka)) (Conway et al., 1999; Bentley et al., 2014). The WAIS, and other parts of the AIS, may also be susceptible to retreat and collapse during warm interglacials (Scherer et al., 1998; McKay et al., 2012; Dutton et al., 2015; Steig et al., 2015; DeConto & Pollard, 2016; Wilson et al., 2018).

The size and configuration of the Antarctic Ice Sheet (AIS) varies in response to mass balance processes (Scambos et al., 2017). These include ice melt, accumulation and ice flow (e.g. Pollard & DeConto, 2009; DeConto & Pollard, 2016; Scambos et al., 2017). For the WAIS, the melt and calving rates may be the most important. These processes are partly sensitive to sea water temperature, alongside atmospheric circulation changes. In contrast, mass and elevation changes in the East Antarctic Ice Sheet (EAIS) may be driven mainly by variations in the rate of accumulation (Ritz et al., 2001).

Studies investigating the global climate response of lowering AIS (e.g. Mechoso, 1980, 1981; Parish et al., 1994; Singh et al., 2016) report consistent conclusions: enhanced poleward energy transport, leading to an adiabatic warming over the continent and a cooling over the Southern Ocean and lower latitudes, one exception is Justino et al. (2014). This change in the thermal atmospheric gradient creates a weakening and northward shift in storm tracks, and thus decreases in poleward eddy moisture transport. AIS flattening also reduces the katabatic winds. All these results are expected to have a significant impact on the composition of water stable isotopes in the precipitation.

The last interglacial period (LIG; between approximately 130 and 115 ka) is associated with warmer-than-present Antarctic air temperatures, inferred from a peak in ice core isotope records at ∼128 ka, and a global sea level rise of 6-9 m above sea level compared to present (Kopp et al., 2009, 2013), suggesting a reduced AIS (Dutton et al., 2015). The LIG period is characterized by an enigmatic mismatch between model experiments and Antarctic ice core data. Changes in AIS elevation have been suggested as one hypothesis to explain the model-data discrepancy (e.g. Bradley et al., 2012; Holloway et al., 2016, 2018). Isolating the elevation signal could provide constraints on future AIS behaviour and thus the future Antarctic contribution to sea level.

The LIG represents a time when AIS changes are relevant for future AIS loss scenarios (e.g. DeConto & Pollard, 2016). Water stable isotope signals recorded in ice cores provide information on past changes spanning glacial-interglacial cycles (e.g. EPICA, 2004). However, past studies with the exception of Werner et al. (2018), have tended to concentrate on temperature, rather than AIS changes.

Here we investigate the stable water isotope (δ^{18}O) response to changes in AIS elevation using an ensemble of isotope-enabled climate model experiments with the HadCM3 model. We describe the patterns of surface air temperature (SAT), precipitation and precipitated δ^{18}O in response to elevation changes, and compare isotope-elevation relationships at the continental scale as well as at the location of ice cores spanning the LIG. Finally, we briefly discuss our results regarding the state of the art of AIS changes related studies, as well as the current interpretation of the LIG isotopic signatures.

2 Materials and Methods

The isotopic response to idealised changes in AIS elevation are simulated using the isotope-enabled coupled ocean–atmosphere–sea-ice General Circulation Model, HadCM3 (Tindall et al., 2009). Two control simulations were used: a preindustrial (PI) simulation, and a 128 ka simulation centred on the LIG Antarctic isotope maximum including a modern day AIS configuration (Holloway et al., 2016). Then a suite of eight idealised AIS elevation change simulations were performed (Supplementary Information Table 1) using orbital and greenhouse-gas forcing at 128 ka. Each experiment scaled the AIS and relates the change to elevation at the EPICA Dome C (EDC) ice core site following:

$$\beta = \frac{Z_{EDC}}{(Z_{EDC} + \Delta z)}, \tag{1}$$

where Z_{EDC} is the EDC ice core site elevation in the modern day AIS configuration, Δz is the prescribed elevation change which extends to ± 1000 m, and β is the scaling coefficient. Elevations across the Antarctic continent are then increased or decreased proportional to β;

$$Z_A^{'} = Z_A/\beta \tag{2}$$

where Z_A is the two-dimensional array of modern AIS elevations and $Z_A^{'}$ is a new array of altered AIS elevations. This approach maintains the modern shape of the AIS, thus reducing the influence of changing ice sheet configuration on circulation and climate and isolating the effect of elevation changes alone. We perform experiments with Δz equal to (+/-) 100, 200, 500 and 1000 m. Each of the above elevation change scenarios is integrated for a total of 500-years to ensure that surface and mid-depth climate fields are sufficiently spun-up with the imposed elevation changes. The last 50 years of each simulation are analysed.

LIG Antarctic isotope maximum of between +2-4 ‰above PI in δ^{18}O are recorded in East Antarctic ice cores. We evaluate our elevation scenarios against LIG δ^{18}O maxima from five published ice core records from East Antarctica (Masson-Delmotte et al., 2011): Vostok (Petit et al., 1999), Dome Fuji (DF, Kawamura et al., 2007), EPICA Dome

C (EDC, Jouzel et al., 2007), EPICA Dronning Maud Land (EDML, EPICA Community Members, 2006) and Talos Dome Ice Core (TALDICE, Stenni et al., 2011). The records are processed following the approach outlined in Holloway et al. (2017): The ice core isotope records are synchronised to the EDC3 age scale (Parrenin et al., 2007) and interpolated onto a common 100 year time grid. Any residual temporal misalignment between the ice cores is minimised by applying a 1500 yr low-pass filter to each record before taking the LIG peak (Sime et al., 2009). Fractional isotopic content is expressed for oxygen-18 as:

$$\delta^{18}O = 1,000 \times \frac{\frac{H_2^{18}O}{H_2^{16}O}}{R_{VSMOW} - 1} \tag{3}$$

in ‰, where R_{VSMOW} is the ratio of $H_2^{18}O$ to $H_2^{16}O$ for Vienna standard mean ocean water.

For all our statistical analyses, averages are given with its associated standard deviation (average ± standard deviation). Linear relationships are considered significant when the p-value is lower than 0.05.

3 Results

3.1 Changes in temperature, precipitation, and δ^{18}O

The LIG forcing, with no additional AIS elevation change, induces a warming of 0.9 ± 0.0 °C compared to PI (Supporting information, Table 2): the continental pattern of warming is similar to an homogeneous warming over the continent with larger changes in the Southern Ocean, especially over the Amundsen Sea and the Indian Ocean. Antarctic precipitation increases by 0.6 ± 0.2 mm/month (on average). The changes are larger in the coastal regions and show wider regional difference: precipitation increases on the coast of the Bellingshausen Sea but decreases on the coast of the Amundsen Sea (c.f. Otto-Bliesner et al., 2020). The Antarctic δ^{18}O in precipitation increases by 0.6 ± 0.4 ‰change.

Increases in AIS elevation act to decrease SAT, confirming findings by Mechoso (1980, 1981); Parish et al. (1994); Singh et al. (2016). The mean Antarctic temperature is 4.5 ± 4.1 °C higher for the DC-1km experiment, while it is 4.4 ± 3.9 °C lower for the DC+1km experiment, compared to the LIG simulation. Larger changes of SAT occur on coastal areas compared to the plateau (Supporting information, Table 3). It is also interesting that the spatial variability is larger when decreasing the elevation compared to increasing the elevation, and in coastal areas. As an example, above 3000 m a.s.l, the temperature change with altitude, deduced from the spatial variability, decreases from -11.8 °C/km for the LIG simulation, to -14.0 °C/km for the DC-1km simulation, while between 1000 and 2000 m a.s.l, it decreases from -8.4 °C/km for the LIG simulation to -14.6 °C/km for the DC-1km simulation.

Changes in precipitation tend to match the SAT changes, so precipitation tends to decrease with increasing AIS elevation. Mean Antarctic precipitation anomalies compared to LIG are 3.1 ± 0.8 mm.month^{-1} for the DC-1km experiment, and -2.4 ± 0.7 mm.month^{-1} for the DC+1km experiment. Nevertheless, differences between the patterns in SAT and precipitation do occur. The largest precipitation changes ($\prec$-5 mm.month^{-1}, and $\succ$5 mm.month^{-1}), for the DC+1km and DC-1km experiments respectively occur in East coastal areas where the orographic slope is the highest. This is consistent with the highest DC-1km precipitation increases occurring along the coasts facing the Indian Ocean, the Weddell Sea and along the Ronne Ice Shelf, where the orographic slopes are the steepest (c.f. Krinner & Genthon, 1999). The Eastern part of the Peninsula and the WAIS coast display opposite trends, i.e. increasing (decreasing) precipitation with increasing (decreasing) AIS elevation. This is likely due to differing western heat fluxes associated with a more stationary Amundsen Sea low when AIS topography is lower (Krinner & Genthon, 1999).

At the continental scale, δ^{18}O does not seem to vary directly together with the elevation, but rather appears to change in response to SAT (see Figure 1). We observe a decrease (increase) in δ^{18}O with the AIS increase (decrease) of 5.9 ± 2.7 ‰for the DC+1km simulation compared to the LIG simulation (-2.9 ± 1.1 ‰for the DC-1km simulation compared to the LIG). However, at the meso-scale, heterogenous patterns stand out, independently from the LIG forcing, with intensified changes mainly in East Antarctica. These changes seem to follow mean sea level pressures isobars (grey lines, e.g. for the DC+500m experiment).

3.2 The impact of sea ice

Antarctic sea ice extent increases by 7.6 % for the DC-1km experiment, whereas it decreases when the AIS elevation increases, by -10.8 % for the DC+1 km experiment (Figure 1). This sea ice against AIS size relationship was identified by Singh et al. (2016) for the case of a 10 % flattening of AIS compared to PI.

Their study shows changes in surface wind stress, and especially strenghtening south of 60 °S resulting in a Northward Ekman transport through changes in westerly momentum transfer and subsequent sea-ice extent. Our simulations display less distinct features. Surface wind speeds, and especially South westerly winds hardly decrease with AIS decrease (Supporting information, Figure 1), and are not shifted. However, similar Meridional Oceanic Circulation (MOC) changes can be observed (Supporting information, Figure 2), with a weakening of low latitudes warm currents towards Antarctica. The simulations of Steig et al. (2015) found the same changes in MOC (though weaker), but decreasing of sea ice extent with WAIS decrease–opposite in sign to that of Singh et al. (2016). Thus, the sign of sea ice change depends on the details of the topographic change.

These changes are spatially nonuniform. The Antarctic sea ice extent changes are the highest, by far, for the Bellingshausen sector with a 50 % increase for the DC+1km experiment (Supporting information, Table 4 and Figure 3). This is likely also related to differing western heat fluxes associated with a more stationary Amundsen Sea low when AIS topography is lower (Krinner & Genthon, 1999). The Weddell sector shows the lowest changes (± 5 %). Other sectors remain in a ± 15 % range. The Bellingshausen and Weddell sectors also stand out by not linearly decreasing with the elevation compared to other sectors, which decrease by a -1 % 100 m^{-1} at Dome C on average (with a mean correlation coefficient of 0.93 and a p-value less than to 0.05).

In terms of controls on temperature, precipitation, δ^{18}O, these sea ice changes are small compared with the changes in sea ice explored in Holloway et al. (2016). This is confirmed in Supporting information, Figure 4. Indeed, removing the impacts of sea ice on using the linear relationship shown in this Supporting Information Figure 4 indicates that there is a very small effect on precipitation (-3.0 ± 1.7 % and 4.4 ± 2.4 % changes compared to the LIG for the DC+1km and DC-1km simulations respectively), ΔSAT (0.4 ± 0.5 % and -0.5 ± 0.7 % changes compared to the LIG for the DC+1km and DC-1km simulations respectively) and $\Delta\delta^{18}$O (0.9 ± 0.4 % and -1.4 ± 0.6 % changes compared to the LIG for the DC+1km and DC-1km simulations respectively). It is of interest in understanding Antarctic LIG measurements that these indirect AIS-sea ice mediated impacts on temperature, precipitation, and δ^{18}O are small, and is on interest in itself in terms of understanding controls on sea ice (Chadwick et al., 2020; Holloway et al., 2017). Since the impacts are small, we herein consider them an intrinsic part of the response to AIS change.

3.3 Linear temperature and δ^{18}O versus elevation relationships

Linear relationships between ΔSAT, ΔP and $\Delta\delta^{18}$O with AIS elevation were calculated using all simulations for each grid point (Figure 2). We find that the Ross Sea and Amundsen Sea and the coastal regions ($\prec$ 1000 m a.s.l) show no significant relationship, possibly because the inter-simulation noise in these quantities is larger than the signal due to the small elevation changes across these regions in our simulations. Outwith these regions, where elevation changes are larger, gradients increase from the coast to the plateau. Mean gradients for ΔSAT versus elevation are -0.34 $\pm$ 0.21 °C/100m for regions between 1000 and 2000 m a.s.l, and -0.92 $\pm$ 0.11 °C/100m for regions above 3000 m a.s.l (Supporting information, Table 5). Singh et al. (2016) report a warming accompanying the reduction of the AIS due to the baroclinic instability over central Antarctica, and the cessation of the katabatic winds on coastal regions, as well as the decreased cyclogenesis over the Southern Ocean. These features could explain the weaker linear relationships on the plateau. Note that correlation coefficients for ΔSAT are higher than 0.9 for all the grid points with significant relationships. ΔP and $\Delta\delta^{18}$O versus elevation have lower correlation coefficients ($\leq$0.8), especially on the plateau. Contrary to ΔSAT, gradients are higher for the coast regions compared to the plateau. The $\Delta\delta^{18}$O versus elevation gradients are spatially noisier than for ΔSAT and ΔP; we estimate that they vary from -0.53 $\pm$ 0.15 ‰/100m for regions above 3000 m a.s.l to -0.92 ‰/100m for regions between 1000 and 2000 m a.s.l.

Interestingly, all ice core locations display linear relationships with ΔSAT, with the exception of Skytrain which has only a small local change in altitude (Figure 2 and Figure 3). Among these ice core locations, two distinct groups can be distinguished by the range of the gradients and the amplitude of changes, the plateau ice cores (EDML, Vostok, EDC and Dome F) with an average gradient of -0.97 $\pm$ 0.09 °C/m, and the other locations (Taylor Dome, Taldice, WAIS Divide and Hercules Dome) with an average of -0.42 $\pm$ 0.0 °C/m. This suggests different processes at play in the Antarctic regions, as shown by ΔSAT of the locations the closest to the Bellingshausen and Weddell sea-ice, and consistent with previous studies (Singh et al., 2016).

The relationships between ΔP and the elevation, and $\Delta\delta^{18}$O with elevation, is better fitted by a 2-degrees polynomial (dashed lines, Figure 3 and Supporting Information Figure 5) for ice cores located on the plateau. For the other sites (with the exception of WAIS Divide and Hercules Dome for decreasing elevations, and Taldice and Taylor Dome for increasing elevations), we nevertheless obtain two significant linear regressions when splitting increase and decrease in elevations ($r^2 \geq$0.95, p$\leq$0.05, Table 6 in the supporting information). Skytrain stands out with a much steeper slope of -5.01 %/100m compared to a mean values -0.31 $\pm$ 0.20 %/100m for the other ice core locations, probably because of its very coastal position.

In contrast to ΔSAT and ΔP, the amplitudes of changes of $\Delta\delta^{18}$O–elevation gradients are not the highest for sites located on the plateau (Supporting information, Table 5). They reach the highest values when decreasing elevations up to a mean of 9.29 $\pm$ 1.19 ‰for the DC+1km experiment, whereas coastal sites reach a 6.13 $\pm$ 1.41 ‰mean value. But they do not display the lowest changes when increasing elevation, of -1.29 $\pm$ 0.91 ‰compared to -3.88 $\pm$ 1.17 ‰mean values for the coastal sites. Skytrain, once more stands out with a much steeper gradient of -3.52 ‰/100m compared to an average of -0.68 $\pm$ 0.17 ‰/100m.

Using our $\Delta\delta^{18}$O–elevation gradients that we applied to δ^{18}O LIG ice core maxima, we find that if all the change in δ^{18}O had to be explained by elevation, it would require an AIS lowering between 200 of 500 m relative to EDC.

4 Conclusions

A flatter AIS size increases sea ice due to changes in atmospheric energy transport and subsequent oceanic transport (Singh et al., 2016). Antarctic sea ice extent increases by 7.6 % for the DC-1km experiment, whereas it decreases when the AIS elevation increases, by -10.8 % for the DC+1 km experiment. The sea ice changes are however spatially nonuniform: the Bellingshausen sector experiences a 50 % increase in sea ice area for the DC+1km experiment, whilst the Weddell sector experiences neglible sea ice changes. We find only a very modest impact of sea ice on δ^{18}O due to elevation-sea ice feedbacks. The (feedback) impact of sea ice on the δ^{18}O-elevation gradients is generally less than 1.4 ± 0.6 %. This supports the idea that we can look at the controls of sea ice and AIS change on ice core measurements independently (Holloway et al., 2016, 2017).

When we use these experiments to look at AIS impacts on δ^{18}O, we show that the response of SAT,P and δ^{18}O to AIS elevations is linear, with the exception of the Ross Sea and Amundsen Sea and the coastal regions ($\leq$1000 m a.s.l). However this lack of relationship in low coastal regions may be an artifact of this model and these simulations. Where simulated elevation changes are larger, gradients increase from the plateau to the coast: $\Delta\delta^{18}$O-elevation gradients are -0.53 ± 0.15 ‰/100m for regions above 3000 m a.s.l to -0.92 ‰/100m for regions between 1000 and 2000 m a.s.l. These different slopes reflect different processes behind AIS elevation-induced δ^{18}O changes, potentially associated with barobaroclinic instability over the plateau, and the cessation of the katabatic winds on coastal regions. Accordingly, all ice core locations display linear relationships with $\Delta\delta^{18}$O and ΔSAT against elevation, with the exception of Skytrain.

Overall, we see that δ^{18}O follows SAT more closely than site elevation change. Larger changes of SAT occur on coastal areas compared to the plateau per m of elevation change. Whilst both δ^{18}O and precipitation tend to follow SAT changes, when site elevation changes, differences do occur in East coastal areas where the orographic slope is high, and the Eastern part of the Peninsula and the WAIS coast display opposite trends, i.e. increasing (decreasing) precipitation with increasing (decreasing) AIS elevation. This suggests we need to employ caution and may need to model δ^{18}O and other ice core species according to accurate WAIS change scenarios to understand how WAIS change will imprint on WAIS cores. That said, if we (likely incorrectly) did assume that the full LIG anomaly in δ^{18}O had to be explained by site elevation changes alone, this would require an AIS lowering between 200 of 500 m relative to EDC. Since Holloway et al. (2016, 2017); Chadwick et al. (2020) suggest however that sea ice also explains a substantial part of the LIG anomaly in δ^{18}O, while Stone et al. (2016) suggest an influence of meltwater and changing AMOC strength, we are not suggesting that this AIS lowering is correct.

Currently confidently dated ice core measurements covering the LIG are only available from East Antarctic core sites. Thus, alongside further δ^{18}O modelling, there is a need for new well dated cores covering the LIG from non-EAIS sites. New ice cores drilled in the WAIS, particularly at Skytrain, or Hercules Dome would be of considerable interest for future AIS LIG reconstructions. Future work to check findings from HadCM3 using more isotope-enabled general climate models would also help to better to constrain the LIG AIS and climate changes.

Acknowledgments

S.G., E.W.W, and L.C.S were funding through the European Research Council under the Horizon 2020 research and innovation programme (grant agreement No 742224, WACSWAIN). E.W.W. is also supported by a Royal Society Professorship. L.C.S. and M.H.acknowledges support through NE/P013279/1, NE/P009271/1, and EU-TiPES. The project has received funding from the European Unions Horizon 2020 research and innovation programme under grant agreement No 820970. This material reflects only the authors views and the Commission is not liable for any use that may be made of the information contained therein. The archiving of the climate model data are underway to be deposit in an appropriate repository of the UK Polar Data Centre (UK PDC). The UK PDC will provide access to the data under the Open Government License (http://www.nationalarchives.gov.uk/doc/open-government-licence/version/3/) and a DOI will be provided.

References

Bentley, M. J., Cofaigh, C. ., Anderson, J. B., Conway, H., Davies, B., Graham, A. G., ... Zwartz, D. (2014). A community-based geological reconstruction of antarctic ice sheet deglaciation since the last glacial maximum. *Quaternary Science Reviews*, *100*, 1 - 9. Retrieved from `http://www.sciencedirect.com/science/article/pii/S0277379114002546` (Reconstruction of Antarctic Ice Sheet Deglaciation (RAISED)) doi: https://doi.org/10.1016/j.quascirev.2014.06.025

Bradley, S. L., Siddall, M., Milne, G. A., Masson-delmotte, V., & Wolff, E. (2012). Where might we find evidence of a Last Interglacial West Antarctic Ice Sheet collapse in Antarctic ice core records? *Global and Planetary Change*, *88-89*, 64–75. doi: 10.1016/j.gloplacha.2012.03.004

Chadwick, M., Allen, C., Sime, L., & Hillenbrand, C.-D. (2020). Analysing the timing of peak warming and minimum winter sea-ice extent in the southern ocean during mis 5e. *Quaternary Science Reviews*, *229*, 106134.

Conway, H., Hall, B. L., Denton, G. H., Gades, A. M., & Waddington, E. D. (1999). Past and future grounding-line retreat of the west antarctic ice sheet. *Science*, *286*(5438), 280–283. Retrieved from `http://science.sciencemag.org/content/286/5438/280` doi: 10.1126/science.286.5438.280

DeConto, R. M., & Pollard, D. (2016). Contribution of antarctica to past and future sea-level rise. *Nature*, *531*(7596), 591–597.

Dutton, A., Carlson, A. E., Long, A. J., Milne, G. A., Clark, P. U., DeConto, R., ... Raymo, M. E. (2015). Sea-level rise due to polar ice-sheet mass loss during past warm periods. *Science*, *349*(6244). Retrieved from `http://science.sciencemag.org/content/349/6244/aaa4019` doi: 10.1126/science.aaa4019

EPICA, C. (2004). Eight glacial cycles from an Antarctic ice core. *Nature*, *429*, 623–628. (doi:10.1038/nature02599)

EPICA Community Members. (2006). One-to-one coupling of glacial climate variability in Greenland and Antarctica. *Nature*, *444*(7116), 195–198. Retrieved from `http://www.nature.com/doifinder/10.1038/nature05301` doi: 10.1038/nature05301

Holloway, M. D., Sime, L. C., Allen, C. S., Hillenbrand, C. D., Bunch, P., Wolff, E., & Valdes, P. J. (2017). The Spatial Structure of the 128 ka Antarctic Sea Ice Minimum. *Geophysical Research Letters*, *44*. doi: 10.1002/2017GL074594

Holloway, M. D., Sime, L. C., Singarayer, J. S., Tindall, J. C., Bunch, P., & Valdes, P. J. (2016, aug). Antarctic last interglacial isotope peak in response to sea ice retreat not ice-sheet collapse. *Nature Communications*, *7*, 12293. Retrieved from `http://dx.doi.org/10.1038/ncomms12293http://10.0.4.14/ncomms12293http://www.nature.com/articles/ncomms12293{\#}supplementary-information`

Holloway, M. D., Sime, L. C., Singarayer, J. S., Tindall, J. C., & Valdes, P. J. (2018). Simulating the 128 ka Antarctic climate response to Northern Hemisphere ice sheet melting using the isotope-enabled HadCM3. *Geophysical Research Letters*, *??*. doi: 10.1029/2018GL079647

Jouzel, J., Masson-Delmotte, V., Cattani, O., Dreyfus, G., Falourd, S., Hoffmann, G., ... Wolff, E. W. (2007, aug). Orbital and millennial Antarctic climate variability over the past 800,000 years. *Science*, *317*(5839), 793–796. Retrieved from `http://www.ncbi.nlm.nih.gov/pubmed/17615306` doi: 10.1126/science.1141038

Justino, F., Marengo, J., Kucharski, F., Stordal, F., Machado, J., & Rodrigues, M. (2014). Influence of antarctic ice sheet lowering on the southern hemisphere climate: modeling experiments mimicking the mid-miocene. *Climate dynamics*, *42*(3-4), 843–858.

Kawamura, K., Parrenin, F., Lisiecki, L., Uemura, R., Vimeux, F., Severinghaus, J. P., ... Watanabe, O. (2007). Northern Hemisphere forcing of climatic cycles in Antarctica over the past 360,000 years. *Nature*, *448*(7156), 912–916. doi: 10.1038/nature06015

Kopp, R. E., Simons, F. J., Mitrovica, J. X., Maloof, A. C., & Oppenheimer, M. (2009). Probabilistic assessment of sea level during the last interglacial stage. *Nature*, *462*, 863–868. doi: 10.1038/nature08686

Kopp, R. E., Simons, F. J., Mitrovica, J. X., Maloof, A. C., & Oppenheimer, M. (2013). A probabilistic assessment of sea level variations within the last interglacial stage. *Geophysical Journal International*. doi: 10.1093/gji/ggt029

Krinner, G., & Genthon, C. (1999). Altitude dependence of the ice sheet surface climate. *Geophysical research letters*, *26*(15), 2227–2230.

Masson-Delmotte, V., Buiron, D., Ekaykin, a., Frezzotti, M., Gallée, H., Jouzel, J., ... Vimeux, F. (2011, apr). A comparison of the present and last interglacial periods in six Antarctic ice cores. *Climate of the Past*, *7*(2), 397–423. Retrieved from `http://www.clim-past.net/7/397/2011/` doi: 10.5194/cp-7-397-2011

McKay, R., Naish, T., Powell, R., Barrett, P., Scherer, R., Talarico, F., ... Williams, T. (2012). Pleistocene variability of antarctic ice sheet extent in the ross embayment. *Quaternary Science Reviews*, *34*, 93–112. Retrieved from `http://www.sciencedirect.com/science/article/pii/S0277379111004057` doi: https://doi.org/10.1016/j.quascirev.2011.12.012

Mechoso, C. R. (1980). The atmospheric circulation around antarctica: Linear stability and finite-amplitude interactions with migrating cyclones. *Journal of the Atmospheric Sciences*, *37*(10), 2209–2233.

Mechoso, C. R. (1981). Topographic influences on the general circulation of the southern hemisphere: A numerical experiment. *Monthly Weather Review*, *109*(10), 2131–2139.

Otto-Bliesner, B., Brady, E., Zhao, A., Brierley, C., Axford, Y., Capron, E., ... others (2020). Large-scale features of last interglacial climate: Results from evaluating the lig127k simulations for cmip6-pmip4. *Climate of the Past Discussions*.

Parish, T. R., Bromwich, D. H., & Tzeng, R.-Y. (1994). On the role of the antarctic continent in forcing large-scale circulations in the high southern latitudes. *Journal of the atmospheric sciences*, *51*(24), 3566–3579.

Parrenin, F., Dreyfus, G., Durand, G., Fujita, S., Gagliardini, O., Gillet, F., ... Kawamura, K. (2007). 1-D-ice flow modelling at EPICA Dome C and Dome Fuji , East Antarctica. *Climate of the Past*, *3*, 243–259.

Petit, J. R., Raynaud, D., Basile, I., Chappellaz, J., Davisk, M., Ritz, C., ... Saltzmank, E. (1999). Climate and atmospheric history of the past 420,000 years from the Vostok ice core, Antarctica. *Nature*, *399*, 429–436.

Pollard, D., & DeConto, R. M. (2009, mar). Modelling West Antarctic ice sheet growth and collapse through the past five million years. *Nature*, *458*(7236), 329–32. Retrieved from http://www.ncbi.nlm.nih.gov/pubmed/19295608 doi: 10.1038/nature07809

Ritz, C., Rommelaere, V., & Dumas, C. (2001). Modeling the evolution of Antarctic ice sheet over the last 420,000 years' Implications for altitude changes in the Vostok region. *JOURNAL OF GEOPHYSICAL RESEARCH*, *106*(D23), 943–974. doi: 10.1029/2001JD900232

Scambos, T., Bell, R., Alley, R., Anandakrishnan, S., Bromwich, D., Brunt, K., ... Yager, P. (2017). How much, how fast?: A science review and outlook for research on the instability of antarctica's thwaites glacier in the 21st century. *Global and Planetary Change*, *153*, 16–34. Retrieved from http://www.sciencedirect.com/science/article/pii/S092181811630491X doi: 10.1016/j.gloplacha.2017.04.008

Scherer, R. P., Aldahan, A., Tulaczyk, S., Possnert, G., Engelhardt, H., & Kamb, B. (1998). Pleistocene Collapse of the West Antarctic Ice Sheet. *Science*, *281*(5373), 82–85. Retrieved from http://dx.doi.org/10.1126/science.281.5373.82 doi: 10.1126/science.281.5373.82

Sime, L. C., Wolff, E. W., Oliver, K. I. C., & Tindall, J. C. (2009, nov). Evidence for warmer interglacials in East Antarctic ice cores. *Nature*, *462*, 342–345. Retrieved from http://www.ncbi.nlm.nih.gov/pubmed/19924212 doi: 10.1038/nature08564

Singh, H. K., Bitz, C. M., & Frierson, D. M. (2016). The global climate response to lowering surface orography of antarctica and the importance of atmosphere–ocean coupling. *Journal of Climate*, *29*(11), 4137–4153.

Steig, E. J., Huybers, K., Singh, H. A., Steiger, N. J., Ding, Q., Frierson, D. M., ... White, J. W. (2015). Influence of west antarctic ice sheet collapse on antarctic surface climate. *Geophysical Research Letters*, *42*(12), 4862–4868.

Stenni, B., Buiron, D., Frezzotti, M., Albani, S., Barbante, C., Bard, E., ... Udisti, R. (2011, dec). Expression of the bipolar see-saw in Antarctic climate records during the last deglaciation. *Nature Geoscience*, *4*(1), 46–49. Retrieved from http://www.nature.com/doifinder/10.1038/ngeo1026 doi: 10.1038/ngeo1026

Stone, E. J., Capron, E., Lunt, D. J., Payne, A. J., Singarayer, J. S., Valdes, P. J., & Wolff, E. W. (2016). Impact of meltwater on high-latitude early last interglacial climate. *Climate of the Past*, *12*(9), 1919–1932.

Tindall, J. C., Valdes, P. J., & Sime, L. C. (2009, feb). Stable water isotopes in HadCM3: Isotopic signature of El Niño - Southern Oscillation and the tropical amount effect. *Journal of Geophysical Research*, *114*, 12pp. Retrieved from http://www.agu.org/pubs/crossref/2009/2008JD010825.shtml doi: 10.1029/2008JD010825

Werner, M., Jouzel, J., Masson-Delmotte, V., & Lohmann, G. (2018). Reconciling glacial antarctic water stable isotopes with ice sheet topography and the isotopic paleothermometer. *Nature Communications*, *9*(3537).

Wilson, D. J., Bertram, R. A., Needham, E. F., van de Flierdt, T., Welsh, K. J., McKay, R. M., ... Escutia, C. (2018). Ice loss from the east antarctic ice sheet during late pleistocene interglacials. *Nature*, *561*(561), 383–386. Retrieved from https://doi.org/10.1038/s41586-018-0501-8

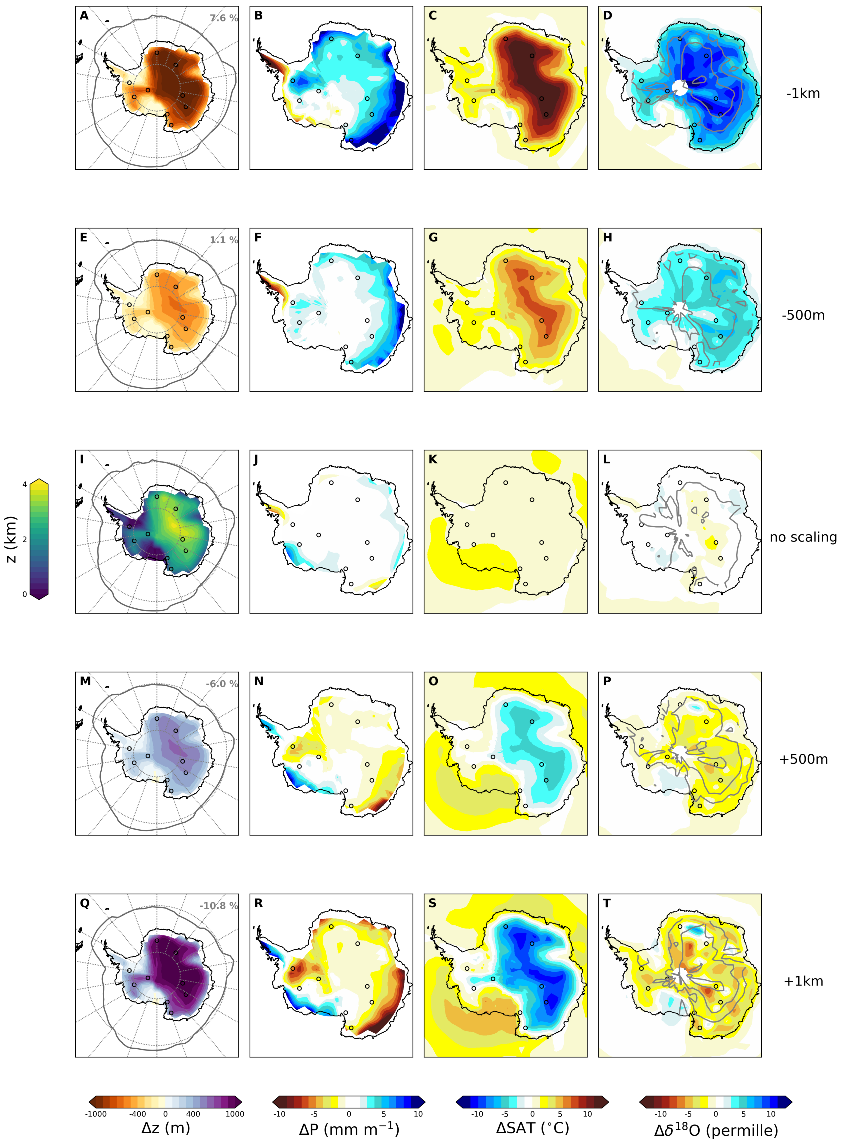

Figure 1. Patterns of idealised Antarctic Ice Sheet simulations. Map of Antarctic elevation change in response to elevation scaling of -1km (first row); -500m (second row); no scaling (third row); +500m (fourth); and +1km (last row), relative to the height at EDC. Pannel I represents the orography of the reference Antarctic configuration (”Z”, in km). The different panels (the exception of panel I) display anomalies relative to a pre-industrial control experiment using the reference Antarctic configuration of (i)the orography (”ΔZ”, in m) with the September sea-ice extent (≥15%, grey contours), precipitation (”ΔP”, in mm/month), surface air temperature (”ΔSAT”, in °C) and δ^{18}O ($\Delta\delta^{18}$O, in ‰) with mean sea level pressure isobars (grey contours, to test matching patterns between isobars and δ^{18}O patterns). September sea-ice anomalies are given in the top right of the figures given the orography and the September sea-ice extent.

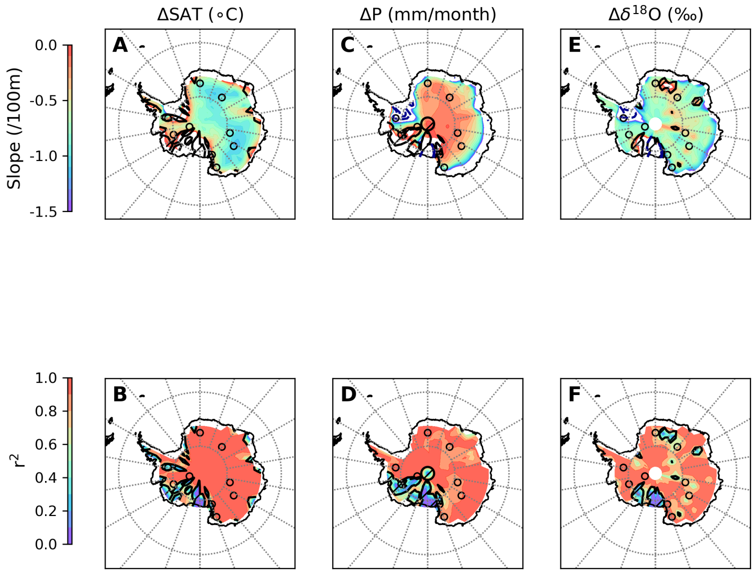

Figure 2. Continental-scale elevation gradients. Slopes ("Slope", pannels A, C and E) and variance ("r^2", pannels B, D and F) between the deviations of simulated surface air temperature ("ΔSAT", slope in °C/100m), precipitation ("ΔP", slope in mm/month/100m) and δ^{18}O in the precipitation ("$\Delta\delta^{18}$O", slope in ‰/100m) compared to the Last Interglacial simulation, and the elevation at each grid point.In the Weddell region, slopes for precipitation and δ^{18}O can be particular low, and are thus shown by blue contours (-20 and -50 ° C/100m for temperature, -20 and -50 mm/month/100m). Non significant relationships are hatched.

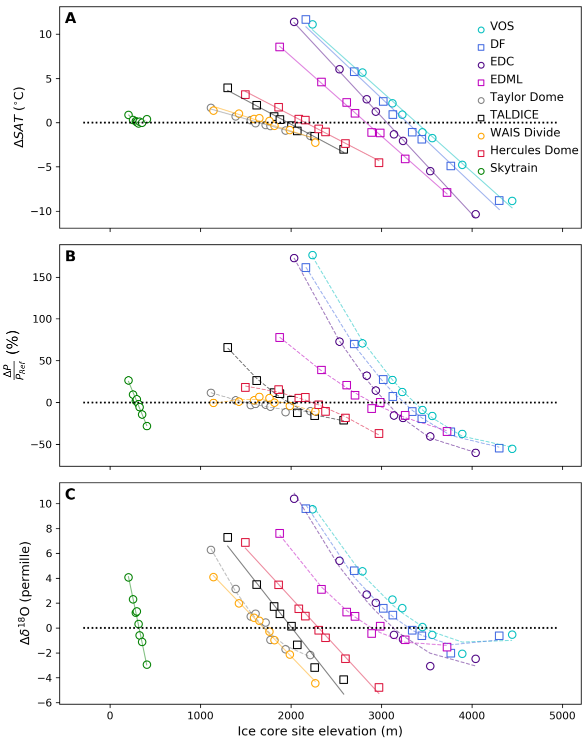

Figure 3. Ice core site elevation gradients. Deviations in ice core (A) surface air tempertaure ("ΔSAT", in °C), (B) precipitation flux ("$\Delta P/P_{Ref}$", in %), and (C) $\delta^{18}O$ ($\Delta\delta^{18}O$, in ‰) compared to the LIG simulation, against the site elevation (in m) for a range of Antarctic ice core sites discussed in the text: Vostok ("VOS"), Dome F ("DF"), EPICA Dome C ("EDC"), EPICA Dronning Maud Land ("EDML"), Taylor Dome ("Taylor Dome"), Talos Dome ("TALDICE"), WAIS Divide ("WAIS Divide"), Hercules Dome ("Hercules Dome") and Skytrain ("Skytrain"). Dots are associated with ice core sites, solid lines emphasize strong linear relationships and dashed lines strong 2-degree polynomials.

Supporting Information for "Antarctic Ice Sheet elevation impacts on water isotope records during the Last Interglacial"

Sentia Goursaud[1], Max Holloway[2], Louise Sime[3], Eric Wolff[1], Paul Valdes[4], Eric Steig[5], Andrew Pauling[5]

[1]Department of Earth Sciences, University of Cambridge, UK

[2]Scottish Association for Marine Science, Oban, UK

[3]Ice Dynamics and Paleoclimate, British Antarctic Survey, Cambridge, UK

[4]School of Geographical Science, University of Bristol, Bristol, UK

[5]Department of Atmospheric Sciences, University of Washington, Seattle, US

Contents of this file

1. Tables S1 to S4
2. Figures S1 to S5

Introduction This supporting information brings extended analyses to those given in the manuscript.

Corresponding author: Sentia Goursaud, Department of Earth Sciences, University of Cambridge, UK (sg952@cam.ac.uk)

Table S1. Model Simulations. Experiment name ("Experiment"), run duration ("Duration" in years), year for the orbital configuation ("Orbit" in kyears BP), and elevation change compared to EDC ("EDC Δz" in meter). All simulations were carried out using HadCM3.

Experiment	Duration (yrs)	Orbit (ka)	EDC Δz (m)
PI	700	0	0
LIG	700	128	0
DC+1km	500	128	+1000
DC+500m	500	128	+500
DC+200m	500	128	+200
DC+100m	500	128	+100
DC-100m	500	128	-100
DC-200m	500	128	-200
DC-500m	500	128	-500

Table S2. Time averaged values over the whole Antarctic. Surface air temperature ("SAT" in ° C), precipitations ("P" in mm/month) and δ^{18}O in the precipitations (in ‰) area-weighted averaged over the last 50 simulated years and the whole Antarctic associated with its standard value.

Experiment	SAT (° C)	P (mm/month)	δ^{18}O (‰)
PI	-36.8 ± 11.8	14.5 ± 15.9	-40.3 ± 12.3
LIG	-35.9 ± 11.8	15.1 ± 16.1	-39.7 ± 12.7
DC+1km	-31.41 ± 7.7	18.1 ± 15.3	-33.8 ± 10.0
DC+500m	-33.5 ± 9.7	16.7 ± 15.8	-36.8 ± 11.5
DC+200m	-34.9 ± 10.9	15.9 ± 15.9	-38.6 ± 12.2
DC+100m	-35.5 ± 11.4	15.4 ± 16.1	-39.1 ± 12.4
DC-100m	-36.4 ± 12.3	14.9 ± 16.3	-40.0 ± 12.8
DC-200m	-36.7 ± 12.6	14.7 ± 16.3	-40.4 ± 12.9
DC-500m	-38.2 ± 13.8	13.9 ± 16.5	-41.6 ± 13.3
DC-1km	-40.3 ± 15.7	12.7 ± 16.8	-42.6 ± 13.3

Table S3. Elevation relationships Area weighted averages and standard deviations of the slopes (”Slope”) and correlation coefficients (”r”) between the deviations of simulated surface air temperature (”SAT” in ° C /100m), precipitations (”P” in mm/month/100m) and δ^{18}O in the precipitations (in ‰/100m) compared to the Last Interglacial simulations and the elevation at each grid point, for different elevation ranges: above 3000 m a.s.l (”≥3000m”), between 2000 and 3000 m a.s.l (”2000-3000m”), between 1000 and 2000 m a.s.l (”1000-2000m”) and below 1000 m a.s.l (”≤1000m”). This table Supplements Figure 2 in the manuscript.

	SAT		P		δ^{18}O	
	Slope	r	Slope	r	Slope	r
¿3000m	-0.92 ± 0.11	-1.0 ± 0.0	-0.22 ± 0.09	-0.96 ± 0.02	-0.53 ± 0.15	-0.83 ± 0.10
2000-3000m	-0.75 ± 0.19	-1.0 ± 0.0	-0.46 ± 0.32	-0.91 ± 0.22	0.70 ± 0.13	-0.94 ± 0.05
1000-2000m	-0.34 ± 0.21	-0.81 ± 0.33	-1.12 ± 1.15	-0.64 ± 0.51	-0.92 ± 0.26	-0.96 ± 0.03
¡1000m	18.65 ± 127.17	0.18 ± 0.75	25.57 ± 249.44	-0.1 ± 0.84	4.66 ± 49.99	-0.6 ± 0.59

Table S4. Changes in the regional sea ice extents Sea ice extent changes (%) when compared to the LIG experiment.The sectors are defined as follows: the Eastern sector (0–180° E), the Weddell sector (60–30° W), the Bellingshausen sector (100–75° W), the Ross sector (180–145° W) and the Pacific sector (180–75° W)

Sector	DC-1km	DC-500m	DC-200m	DC-100m	DC+100m	DC+200m	DC+500m	DC+1km
Bellingshausen	50.0	0.0	0.0	14.3	0.0	0.0	-7.1	0.0
Ross	1.6	1.6	0.0	0.0	-1.6	-1.6	-1.6	-12.5
Pacific	12.8	2.6	0.9	4.3	-1.7	-4.3	-7.7	-16.2
Weddel	-1.2	-3.7	-2.4	3.7	0.0	-2.4	-4.9	-4.9
East	6.9	2.5	0.0	0.0	-1.9	-1.9	-6.9	-10.1
All	7.6	1.1	-0.2	2.3	-1.4	-2.5	-6.0	-10.8

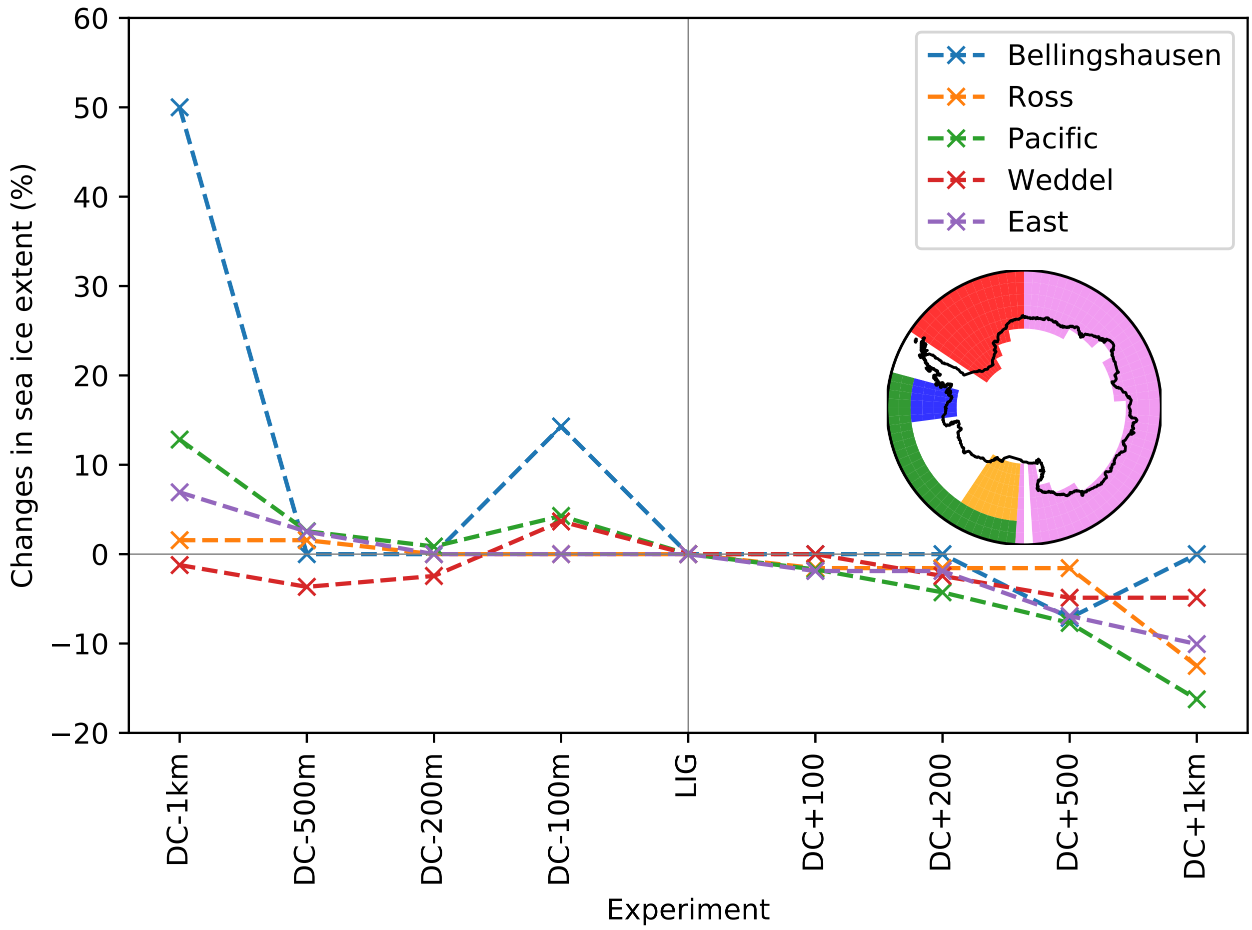

Figure S1. Changes in the regional sea ice extents Changes in sea ice extent (in %) vs changes in elevation (in m) when compared to the BP128 experiment. The sectors are defined as follows: the Eastern sector (0–180° E), the Weddell sector (60–30° W), the Bellingshausen sector (100–75° W), the Ross sector (180–145° W) and the Pacific sector (180–75° W))

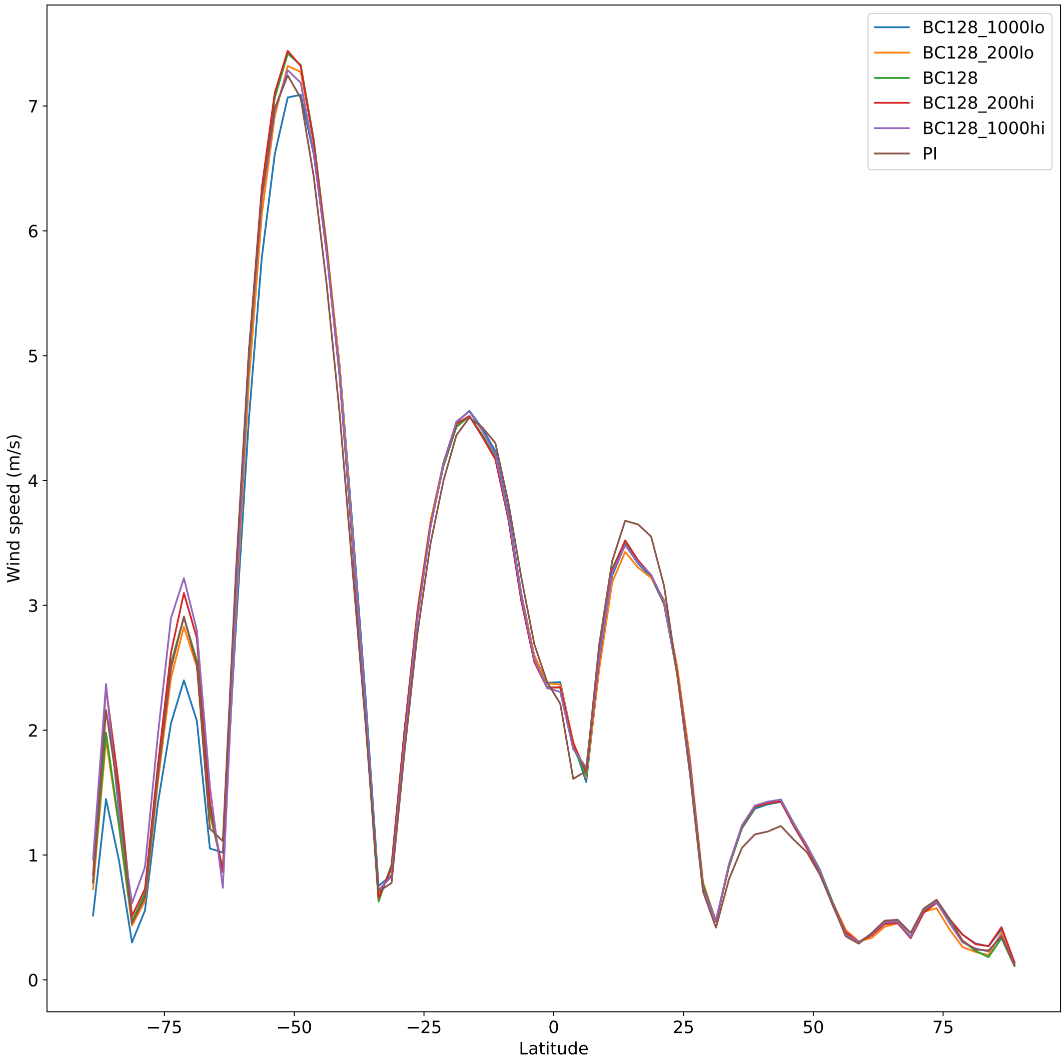

Figure S2. **Surface wind speeds** Surface wind speed (in m/s) vs latitudes for the Preindustrial ("PI", in brown), Last Interglacial ("BC128", in green), DC-1000 ("BC128_1000lo", in blue), DC-200 ("BC128_200lo", in orange), DC+200 ("BC128_200hi", in red), and DC+1000 ("BC128_1000hi", in purple) simulations.

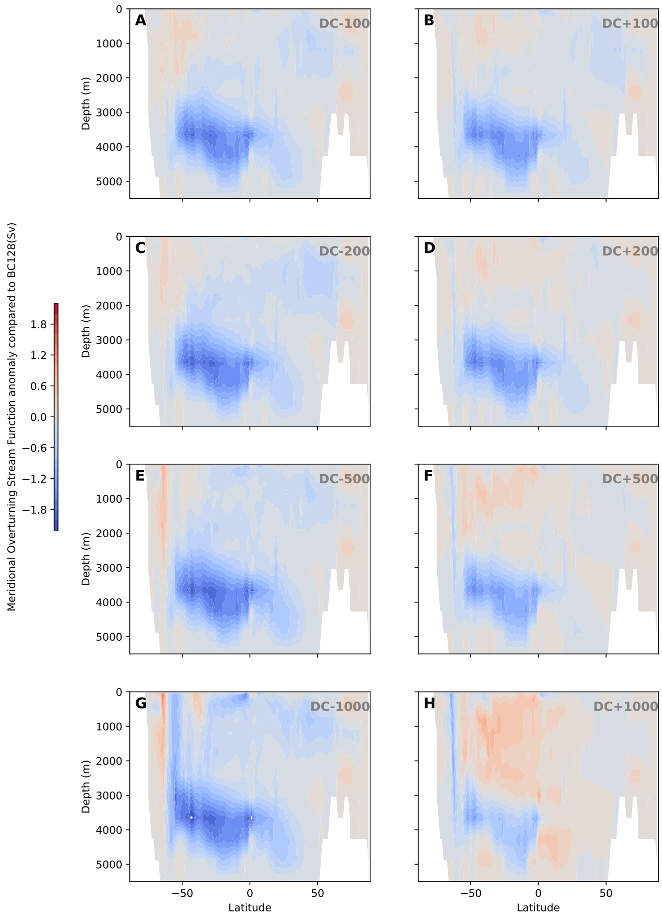

Figure S3. Meridional Overturning Circulation Meriodional Overturning Stream Function anomaly compared to the Last Interglacial (in Sv) along the sea depth (in m) and in function of the latitudes for the DC-100 (pannel A), DC+100 (pannel B), DC-200 (pannel C), DC+200 (pannel D), DC-500 (pannel E), DC+500 (pannel F), DC-1000 (pannel G) and DC+1000 (pannel H) simulations .

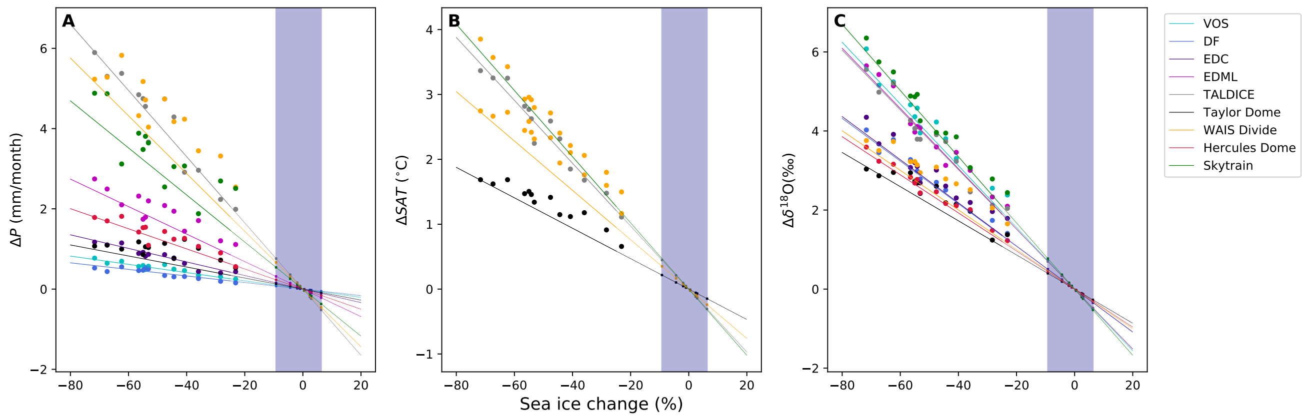

Figure S4. Sea ice corrections Deviations of simulated precipitations (”P” in mm/month, pannel A), surface air temperature (”SAT” in °, pannel B), and δ^{18}O in the precipitations (in ‰, pannel C) compared to the Last Interglacial simulations, against changes in sea ice areas (in %)compared to the Last Inglacial simulations from sea ice reduction sensitivity tests extracted from ? for each ice core location. Dots display outputs form the sea ice reduction sensitivity tests; the lines, the linear regressions for these outputs against the sea ice changes; the blue shadow, the range of our Antarctic Ice Sheet simulations; and little squares the outputs from our Antarctic Ice Sheet simulations.

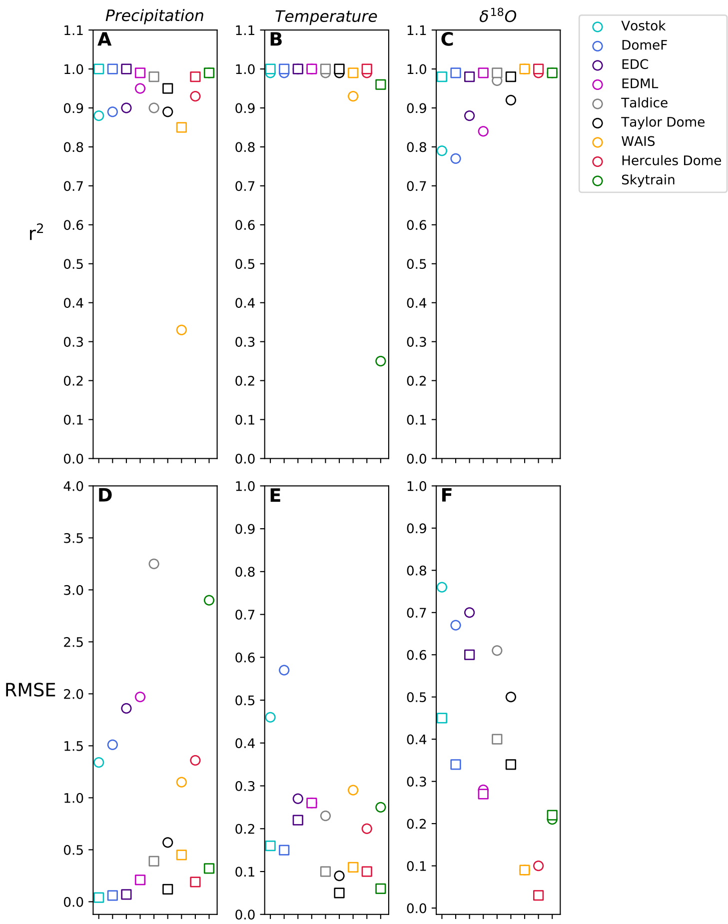

Figure S5. Robustness of ice core elevation linear regressions Correlation coefficient (r^2) (pannels A-C) and RMSE (pannels D-F) of the regressions between the changes in precipitation (pannels A and D), temperature (pannels B and E), $\delta^{18}O$ (pannels C and E) and the changes in elevation for each ice core location. circle markers correspond to linear regressions, while square markers correspond to 2-degrees polynomial regressions.